

Network Model of a 5G MIMO Base Station Antenna in a Downlink Multi-User Scenario

N. Amani¹, R. Maaskant^{1,2}, A. A. Glazunov¹, and M. Ivashina¹

¹Department of Electrical Engineering, Chalmers University of Technology, Gothenburg, Sweden, anavid@chalmers.se, rob.maaskant@chalmers.se, andres.glazunov@chalmers.se, marianna.ivashina@chalmers.se

²Electromagnetics Group, Eindhoven University of Technology (TU/e), The Netherlands, r.maaskant@tue.nl

Abstract—A system level network model of a 5G base station antenna (BSA) with massive multiple-input multiple-output (MIMO) capabilities is presented that incorporates antenna mutual interaction and signal processing aspects. The combined transmitter-channel-receiver in such a system is modeled by cascading \mathbf{Z} -matrices to interrelate the transmitter and receiver port voltages/ currents to one another. The developed model is then subjected to the zero-forcing (ZF) beamforming algorithm to compute the per-antenna transmit power for a specific minimum signal level at the receiver as well as the required BSA effective isotropic radiated power (EIRP). The presented initial results show that in a line-of-sight (LOS) environment the required EIRP to achieve a 1 Gbps bitrate user link in a 15–200 m coverage ranges from 25–48 dBm, which increases to 31–54 dBm after incorporating first-order mutual coupling effects among the BSA elements.

Index Terms—5G, base station antenna, massive multiple-input multiple-output (MIMO), network theory.

I. INTRODUCTION

Future 5G wireless systems are expected to offer Gbps data bitrates to a large number of simultaneous users [1]. To accomplish this arduous goal, the move toward mm-wave frequencies is inevitable and motivated by the need for larger bandwidths. However, the relatively large path loss at those frequencies will require very large effective isotropic radiated power (EIRP) levels on the base station antenna (BSA) side, as well as smaller cell sizes. In addition, transmitting through multiple simultaneous beams will require adaptive beamforming methods for dynamic pattern control [2], based on the channel state information (CSI), which differs from classical array antenna theory where the focus is on the pattern synthesis neglecting mutual coupling and channel effects.

In this paper, a network-theoretic approach is proposed to model a massive MIMO scenario which accounts for both antenna and signal processing effects; (full-wave) mutual coupling effects between the array elements [3], [4], numerical or analytical embedded element patterns and polarimetric effects can readily be included in the model and then be used for signal processing purposes [5]. A line-of-sight (LOS) propagation environment is assumed for the sake of simplicity. Channel fading due to a scattering environment will be factored in at a later stage.

The voltages and currents at the circuit ports of both the BSA array and user equipment (UE) antennas will be

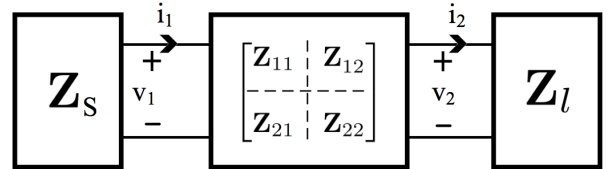


Fig. 1: Network model of a massive MIMO scenario.

interrelated through the impedance—or \mathbf{Z} -matrix—modeling approach. Conservation of energy is enforced to resolve the first-order self and mutual resistances between the transmitting BSA array elements. The far-field coupled signals between the BSA elements and the UE antennas are computed by means of the reaction concept [6].

The so-formed channel matrix provides a useful framework that encompasses the antenna properties and the propagation channel characteristics, which can be subjected to beamforming signal processing algorithms; herein used to compute the per-antenna transmit power for a specific minimum signal level at the receiver as well as the required BSA EIRP.

Regarding the notation, boldface upper case and lower case represents matrices and vectors, respectively, while $(\cdot)^T$ and $(\cdot)^H$ are transpose and Hermitian operators. Field vectors are denoted by overbar (\bar{E}).

Section II describes the network model, Sec. III the numerical results and Sec. IV the Conclusions.

II. NETWORK MODEL OF A MASSIVE MIMO SYSTEM

Figure 1 illustrates the equivalent network model of a massive MIMO for the downlink scenario (i.e. only power amplifiers (PAs) in the BSA). The subscripts 1 and 2 represent the input (BSA) ports and output (UE) ports of this two-port network, respectively. The diagonal matrix \mathbf{Z}_S refers to the source impedance matrix. Assuming M elements at the BSA and K single-antenna UEs, the input/output voltage and current vectors are $\mathbf{v}_1 \in \mathbb{C}^{M \times 1}$, $\mathbf{i}_1 \in \mathbb{C}^{M \times 1}$, $\mathbf{v}_2 \in \mathbb{C}^{K \times 1}$ and $\mathbf{i}_2 \in \mathbb{C}^{K \times 1}$. The matrix representation of the network parameters is given by (1), where $\mathbf{Z}_{11} \in \mathbb{C}^{M \times M}$ is the impedance matrix of the BSA with off-diagonal elements representing the mutual coupling between antenna elements. The matrix $\mathbf{Z}_{22} \in \mathbb{C}^{K \times K}$ refers to the impedance matrix of the UEs,

which we assume to be a diagonal matrix. The LOS wireless channel is modeled using the reaction concept between the radiated E-field pertaining to each element excitation at the open-circuited BSA and each UE antenna current. The so-formed matrix is denoted by $\mathbf{Z}_{12} \in \mathbb{C}^{M \times K}$. Since a reciprocal network/channel is assumed, then $\mathbf{Z}_{12} = \mathbf{Z}_{21}^T$.

$$\begin{bmatrix} \mathbf{v}_1 \\ \mathbf{v}_2 \end{bmatrix} = \begin{bmatrix} \mathbf{Z}_{11} & \mathbf{Z}_{21}^T \\ \mathbf{Z}_{21} & \mathbf{Z}_{22} \end{bmatrix} \begin{bmatrix} \mathbf{i}_1 \\ -\mathbf{i}_2 \end{bmatrix} \quad (1)$$

The entries of the \mathbf{Z}_{12} or \mathbf{Z}_{21} matrices depend on the free space impedance η , wavelength λ , and link distance $r_{km} = \|\bar{\mathbf{r}}_k - \bar{\mathbf{r}}_m\|_2$ between the element k and m . Furthermore, in the far-field, and by using antenna reciprocity, these reactions can be expressed in terms of the antenna far-field function \bar{G} and the antenna input current I as [6]:

$$z_{12(m,k)} = z_{21(k,m)} = \frac{-2j\lambda}{\eta I_k I_m} [\bar{G}_k(\hat{\mathbf{r}}_k) \cdot \bar{G}_m(\hat{\mathbf{r}}_m)] \frac{e^{-jk r_{km}}}{r_{km}} \quad (2)$$

The diagonal matrix \mathbf{Z}_l holding the UE load impedances are related to the network voltages and currents through

$$\mathbf{Z}_l \mathbf{i}_2 = \mathbf{v}_2 \quad (3)$$

Upon expanding (1), and by taking (3) into consideration, we obtain a relationship between the input and output voltage vectors \mathbf{v}_1 and \mathbf{v}_2 , respectively, i.e.,

$$\mathbf{v}_2 = \mathbf{H} \mathbf{v}_1, \quad (4)$$

where \mathbf{H} is the channel matrix, which is expressed in terms of our network parameters as

$$\mathbf{H} = (\mathbf{I} + \mathbf{Z}_{22}(\mathbf{Z}_l)^{-1})^{-1} \mathbf{Z}_{21} (\mathbf{Z}_{11} - \mathbf{Z}_{21}^T (\mathbf{Z}_l + \mathbf{Z}_{22})^{-1} \mathbf{Z}_{21})^{-1}, \quad (5)$$

where \mathbf{I} is a $K \times K$ identity matrix. For the derivation of (5) we refer to Appendix A.

As can be seen from (5), this new $(K + M)$ -port network model of the $K \times M$ channel matrix includes the mutual coupling effects between BSA elements; these are included in \mathbf{Z}_{11} . Furthermore, the polarization and the embedded element patterns are also considered in the far-field functions of the UE and BSA elements [cf. Eq. (2)]. The input-output voltage relationship given by (4) and (5) can now be employed in the analysis of different MIMO beamforming algorithms.

III. SIMULATION RESULTS

In this section, a massive MIMO system operating at 30 GHz is analyzed with the aid of the above-proposed network model. A 30-element uniform linear array (ULA) covering a 120°-wide field of view (FoV) in the azimuthal plane of the BSA is taken. The ZF (pre-coding) beamforming algorithm is employed for the case that two UEs are arbitrarily located within this sector. A constant radiation pattern with non-zero magnitude over the FoV of each of the BSA elements is assumed. We further assume that the BSA elements have the ability to concentrate the radiated power of an isotropic

element [7] in one third of the radiation sphere, i.e., in the region $\pi/6 \leq \phi \leq 5\pi/6$ and $0 \leq \theta < \pi$. Therefore, since the radiated power of the isotropic radiator and the BSA element are equal, i.e. $P_{\text{iso}} = P_{\text{ele}}$, and by realizing that at the far-field point $\bar{\mathbf{r}}$

$$\bar{G}(\bar{\mathbf{r}}) = r e^{jk r} \bar{E}(\bar{\mathbf{r}}), \quad (6)$$

so that $|\bar{G}| \propto |\bar{E}|$ for constant r , we conclude that the far-field function of the isotropic radiator \bar{G}_{iso} and the assumed element \bar{G}_{ele} must have the following relationship on the far-field sphere of the BSA:

$$\int_0^\pi \int_0^{2\pi} |\bar{G}_{\text{iso}}|^2 d\Omega = \int_0^\pi \int_{\pi/6}^{5\pi/6} |\bar{G}_{\text{ele}}|^2 d\Omega$$

$$|\bar{G}_{\text{ele}}|^2 = 3 |\bar{G}_{\text{iso}}|^2 \quad (7)$$

In order to compute the \mathbf{Z}_{11} matrix entries for the assumed BSA element patterns, the conservation of energy law must be satisfied. That is, for lossless antennas, $P_{\text{in}} = P_{\text{rad}}$. This leads to a first-order estimate of the real parts of \mathbf{Z}_{11} :

$$\Re\{Z_{11(m,n)}\} = \frac{1}{\eta} \int_\Omega \bar{E}_m(\bar{\mathbf{r}}) \cdot \bar{E}_n^*(\bar{\mathbf{r}}) r^2 d\Omega \quad (8)$$

where Ω and $\bar{E}(\bar{\mathbf{r}})$ are the solid angle and unit-current-excited BSA embedded element pattern, respectively. A proof of (8) is provided in Appendix B. By assuming a 50- Ω input impedance of an isolated isotropic radiator, \bar{G}_{iso} is determined first and \bar{G}_{ele} is subsequently computed from (7). Next, \bar{G}_{ele} is utilized in the $\Re\{\mathbf{Z}_{11}\}$ -calculation when the proposed elements are employed at the BSA array¹. The first-order self and mutual resistances of the elements in the transmitting BSA array are plotted in Fig. 2.

Furthermore, \bar{G}_{ele} and \bar{G}_{iso} can be used in (2) to compute the \mathbf{Z}_{12} matrix since isotropic radiators are assumed for the UEs. The matrices \mathbf{Z}_{22} and \mathbf{Z}_l are 2×2 diagonal matrices with 50- Ω as diagonal elements thus assuming uncorrelated receivers. After computing all Z-matrices, the channel matrix is calculated through (5) and the ZF precoding is applied at the BS, i.e.,

$$\mathbf{v}_1 = \mathbf{H}^H (\mathbf{H} \mathbf{H}^H)^{-1} \mathbf{v}'_1 \quad (9)$$

In order to compute the actual input voltage vector, a correct normalization for \mathbf{v}'_1 is needed. Inserting (9) in (4) results in the trivial equation $\mathbf{v}_2 = \mathbf{I} \mathbf{v}'_1$.

The resulting output SNR voltage vector at the UEs can be computed given the thermal noise, the receiver noise figure (NF), the channel bandwidth, the digital modulation and the SNR per bit [8]. Here, UEs at room temperature, a 800 MHz channel bandwidth, and a 9 dB NF [9] are assumed for the UEs. Based on [10], for the low symbol error probability of 10^{-6} using 16-QAM, 15 dB SNR per bit is required. Therefore, for 1 Gbps bitrate, the required receiver sensitivity is approximately $\text{RX}_{\text{sen}} = -60$ dBm [8]. Next, the vector \mathbf{v}_1 is evaluated for this specific receiver sensitivity and converted

¹Despite the magnitudes of the BSA element patterns are identical, they need to incorporate the correct phase patterns when displaced from the origin, i.e., $\bar{G}_m = |\bar{G}_m| \exp(-jk \bar{\mathbf{r}}_m \cdot \hat{\mathbf{r}}(\theta, \phi))$.

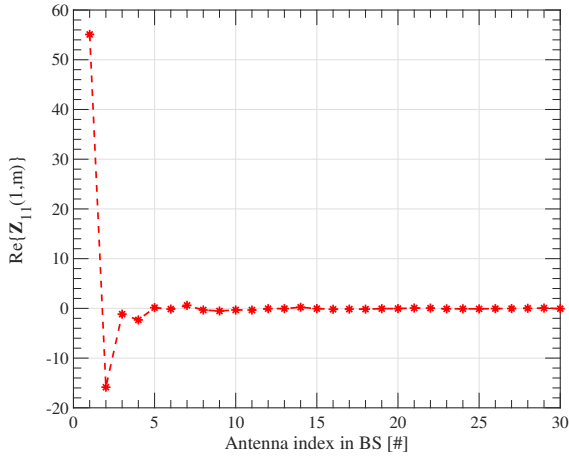


Fig. 2: Self and mutual resistances of the BSA elements, i.e. $\Re\{Z_{11(l,m)}\}$ for $m = 1, \dots, M$.

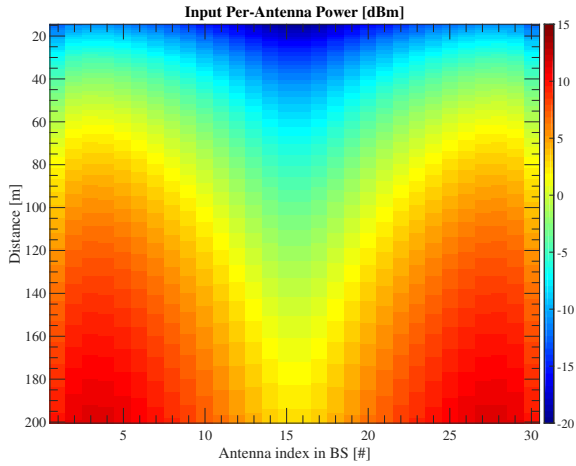


Fig. 3: Per-antenna power distribution at the BSA for different link ranges.

into the actual per-antenna power assuming ZF beamforming towards user k . To this end, the following relationships are used:

$$\mathbf{v}_1 = \mathbf{Z}_{\text{in}} \mathbf{i}_1 \quad (10)$$

where

$$\mathbf{Z}_{\text{in}} = \mathbf{Z}_{11} - \underbrace{\mathbf{Z}_{21}^T (\mathbf{Z}_l + \mathbf{Z}_{22})^{-1} \mathbf{Z}_{21}}_{\text{UE-to-BSA coupling}} \quad (11)$$

and

$$P_{\text{in}(k,m)} = \frac{1}{2} \Re\{v_{k,m} i_{k,m}^*\} \quad (12)$$

and m is the element index at the BSA. In this simulation we consider two UEs located at the same distance to the BSA, 2° apart from each other, i.e., $\theta_1 = 89^\circ$ and $\theta_2 = 91^\circ$ with respect to the end-fire axis of the ULA. The obtained required per-antenna power to form a beam toward UE₁ is plotted in Fig. 3 for different distances between the BSA and the UEs. Since

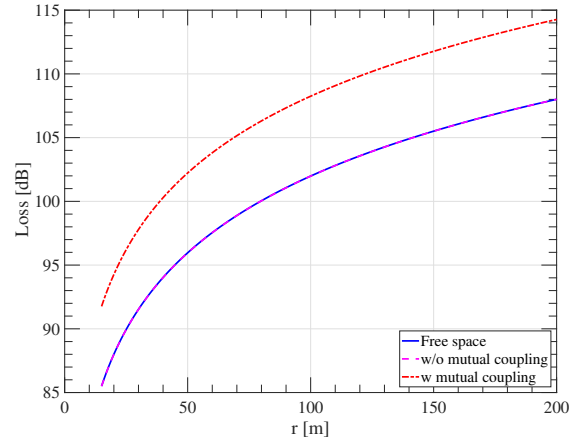


Fig. 4: Expected loss in the proposed model with and without base station antenna mutual interaction at 30 GHz for different link ranges.

the angular distribution of the UEs is preserved for different link ranges, the shape of the power distribution curve is the same². However, as the distance increases the required per-antenna power at the input increases to maintain the link. As can be seen in Fig. 3, taking hardware limitations such as the PA characteristics into account, the BSA configuration (i.e., the number of BSA elements, the inter-element spacing and element type) can be adjusted in order to find a compromise between antenna gain and total input power at the frequency of interest.

Without considering BSA mutual coupling in a pure LOS propagation environment (diagonal matrix \mathbf{Z}_{11}) the experienced loss in the model is equal to the free space path loss. However, including first-order mutual coupling effects in the model introduces an additional loss which is illustrated in Fig. 4. This loss depends on the element radiation pattern and array geometry.

The minimum required EIRP for different link ranges with and without mutual coupling effects are compared in Fig. 5(right). The mutual coupling effect at the BSA array increases the minimum required EIRP by 6 dB.

As already mentioned above, the receiver sensitivity corresponding to the minimum per-antenna power at the BSA depends on the system parameters and targeted bitrate. If the link was designed for a 100 Mbps bitrate, with similar system parameters as mentioned above, the minimum receiver sensitivity would reduce to -70 dBm. The weaker distinguishable signal at the receiver translates to lower per-antenna power at the BSA with the same antenna configuration. Therefore, the minimum required EIRP in the same link designed for 100 Mbps bitrate, illustrated in Fig. 5(left), is expectedly lower in comparison to Fig. 5(right).

²For these BSA power calculations it is assumed that only one user is served at a time, while the other UE is actively suppressed.

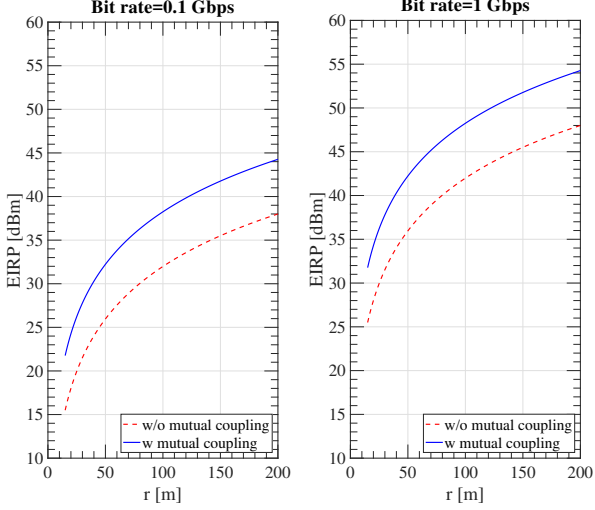


Fig. 5: Minimum required EIRP at 30 GHz for different link ranges designed for 0.1 Gbps bit rate (left) and 1 Gbps bit rate (right) assuming 16-QAM with symbol error probability of 10^{-6} .

IV. CONCLUSION

A network model with the ability to factor realistic antenna effects into the channel matrix has been proposed. The framework enables the design of a BSA array in a massive MIMO downlink scenario. Based on assumed system hardware/software limitations and by using the ZF beamforming algorithm the minimum required per-antenna power and associated EIRP of the BSA have been calculated.

ACKNOWLEDGMENT

This project has received funding from the European Union's Horizon 2020 research and innovation programme under the Marie Skłodowska-Curie grant agreement No 721732.

APPENDIX A

One derives (5) by expanding (1) as

$$\mathbf{Z}_{11}\mathbf{i}_1 - \mathbf{Z}_{21}^T\mathbf{i}_2 = \mathbf{v}_1 \quad (13a)$$

$$\mathbf{Z}_{21}\mathbf{i}_1 - \mathbf{Z}_{22}\mathbf{i}_2 = \mathbf{v}_2 \quad (13b)$$

Then, by calculating \mathbf{i}_2 from (3) and substituting this in (13b), \mathbf{v}_2 can be extracted, i.e.,

$$\mathbf{v}_2 = (\mathbf{I} + \mathbf{Z}_{22}\mathbf{Z}_l^{-1})^{-1}\mathbf{Z}_{21}\mathbf{i}_1. \quad (14)$$

Next, by employing (10) and (11), \mathbf{i}_1 can be expressed as

$$\mathbf{i}_1 = (\mathbf{Z}_{11} - \mathbf{Z}_{21}^T(\mathbf{Z}_l + \mathbf{Z}_{22})^{-1}\mathbf{Z}_{21})^{-1}\mathbf{v}_1 \quad (15)$$

Finally, substituting \mathbf{i}_1 in (14), one readily obtains (5), i.e., $\mathbf{v}_2 = \mathbf{H}\mathbf{v}_1$, where

$$\mathbf{H} = (\mathbf{I} + \mathbf{Z}_{22}(\mathbf{Z}_l^{-1})^{-1})^{-1}\mathbf{Z}_{21}(\mathbf{Z}_{11} - \mathbf{Z}_{21}^T(\mathbf{Z}_l + \mathbf{Z}_{22})^{-1}\mathbf{Z}_{21})^{-1}. \quad (16)$$

Denoting \mathbf{i} and \mathbf{v} as the input current and voltage amplitude vectors, respectively, the total BSA input power P_{in} can be calculated as³

$$P_{\text{in}} = \frac{1}{2}\Re\{\mathbf{i}^H\mathbf{v}\} = \frac{1}{2}\Re\{\mathbf{i}^H\mathbf{Z}_{11}\mathbf{i}\} \quad (17)$$

which can be rewritten as

$$\begin{aligned} P_{\text{in}} &= \frac{1}{4}[\mathbf{i}^H\mathbf{Z}_{11}\mathbf{i} + (\mathbf{i}^H\mathbf{Z}_{11}\mathbf{i})^H] \\ &= \frac{1}{4}[\mathbf{i}^H(\mathbf{Z}_{11} + \mathbf{Z}_{11}^H)\mathbf{i}] \\ &= \frac{1}{2}\mathbf{i}^H\Re\{\mathbf{Z}_{11}\}\mathbf{i} \end{aligned} \quad (18)$$

which must equal the total radiated power.

The total radiated electric field $\bar{\mathbf{E}}(\bar{\mathbf{r}})$ of a transmitting array with open-circuit embedded element pattern $\bar{\mathbf{E}}_m$ and element current excitation i_m is

$$\bar{\mathbf{E}}(\bar{\mathbf{r}}) = \sum_{m=1}^M i_m \bar{\mathbf{E}}_m(\bar{\mathbf{r}}) \quad (19)$$

where $\bar{\mathbf{E}}_m$ is obtained by exciting element m by a unit current amplitude, while open-circuiting the other BSA array elements. A vector representation of (19) is

$$\bar{\mathbf{E}}(\bar{\mathbf{r}}) = \mathbf{e}\mathbf{i} \quad (20)$$

where the column-augmented matrix

$$\mathbf{e} = [\bar{\mathbf{E}}_1(\bar{\mathbf{r}}) \mid \bar{\mathbf{E}}_2(\bar{\mathbf{r}}) \mid \cdots \mid \bar{\mathbf{E}}_M(\bar{\mathbf{r}})]. \quad (21)$$

Then, the total radiated power can be computed as

$$\begin{aligned} P_{\text{rad}} &= \frac{1}{2\eta} \int_{\Omega} |\bar{\mathbf{E}}(\bar{\mathbf{r}})|^2 r^2 d\Omega = \frac{1}{2\eta} \int_{\Omega} |\mathbf{e}\mathbf{i}|^2 r^2 d\Omega \\ &= \frac{1}{2\eta} \int_{\Omega} \mathbf{i}^H \mathbf{e}^H \mathbf{e} \mathbf{i} r^2 d\Omega \\ &= \mathbf{i}^H \underbrace{\frac{1}{2\eta} \int_{\Omega} \mathbf{e}^H \mathbf{e} r^2 d\Omega}_{\text{pattern overlap matrix}} \mathbf{i} \end{aligned} \quad (22)$$

Hence, equality of P_{in} and P_{rad} [i.e. Eq. (18) = Eq. (22)] for a lossless antenna must hold irrespective of \mathbf{i} , which implies that

$$\Re\{\mathbf{Z}_{11}\} = \frac{1}{\eta} \int_{\Omega} \mathbf{e}^H \mathbf{e} r^2 d\Omega, \quad (23)$$

or more specifically,

$$\Re\{Z_{11(m,n)}\} = \frac{1}{\eta} \int_{\Omega} \bar{\mathbf{E}}_m(\bar{\mathbf{r}}) \cdot \bar{\mathbf{E}}_n^*(\bar{\mathbf{r}}) r^2 d\Omega. \quad (24)$$

³For this calculation we assume that $\mathbf{Z}_{\text{in}} = \mathbf{Z}_{11}$ (i.e. loss in \mathbf{Z}_l neglected).

REFERENCES

- [1] Ericsson, "5G systems," *White Paper 284 23-3251 Uen*, 2017. [Online]. Available: <https://www.ericsson.com/assets/local/publications/white-papers/wp-5g-systems.pdf>
- [2] K. F. Warnick and M. A. Jensen, "Network theory and the array overlap integral formulation," 2016. [Online]. Available: <https://ecen665web.groups.et.byu.net/notes/ln11.pdf>
- [3] S. Pratschner, S. Caban, S. Schwarz, and M. Rupp, "A mutual coupling model for massive MIMO applied to the 3GPP 3D channel model," *25th European Signal Processing Conference (EUSIPCO)*, pp. 653–657, 2017.
- [4] J. W. Wallace and M. A. Jensen, "Mutual coupling in MIMO wireless systems: A rigorous network theory analysis," *IEEE Transactions on Wireless Communications*, vol. 3, no. 4, pp. 1317–1325, 2004.
- [5] R. Maaskant, E. Woestenburg, and M. Arts, "A generalized method of modeling the sensitivity of array antennas at system level," in *Microwave Conference, 2004. 34th European*, vol. 3. IEEE, 2004, pp. 1541–1544.
- [6] P.-S. Kildal, *Foundations of antenna engineering: a unified approach for line-of-sight and multipath*. Artech House, 2015.
- [7] H. Yordanov, M. Ivrlač, P. Russer, and J. A. Nossek, "Arrays of isotropic radiators – a field-theoretic justification," in *Proc. ITG/IEEE Workshop on Smart Antennas*, 2009.
- [8] Q. Gu, *RF system design of transceivers for wireless communications*. Springer Science & Business Media, 2005.
- [9] M. Series, "Guidelines for evaluation of radio interface technologies for IMT-advanced," *Report ITU*, no. 2135-1, 2009.
- [10] A. Goldsmith, *Wireless communications*. Cambridge university press, 2005.